

Multi-functional Multi-band Metasurface for Linear and Circular Polarization in Reflection Mode

Abdulkadir Çıldır^{1*}

¹ Vocational College of Technical Sciences, Electronic and Automation, Edirne, Türkiye, (ORCID: 0000-0003-1789-6088), abdulkadir.cildir@trakya.edu.tr

(İlk Geliş Tarihi 06.12.2023 ve Kabul Tarihi 05.02.2024)

(DOI: 10.35354/tbed.1401262)

ATIF/REFERENCE: Çıldır, A. (2024). Multi-functional Multi-band Metasurface for Linear and Circular Polarization in Reflection Mode. *Teknik Bilimler Dergisi*, 14 (1), 26-30.

Abstract

A new metasurface design is presented in multi and broad frequency bands. Metasurface has been designed on Roger 5880 substrate with a thickness of 1.575 mm. The top of the designed metasurface consists of two diagonal mirror m-shaped unit cells. The background plane covers the whole metasurface. Numerical results demonstrate the metasurface's capability for both linear (12.48-13.62 GHz, 19.00-27.64 GHz, 39.45-41.72 GHz, 44.68-45.18 GHz, and 47.52-48.28 GHz) and circular (11.5-12.07 GHz, 30.01-37.77 GHz, 42.3-44.2 GHz, 45.45-47.1 GHz, 48.7-49.54 GHz) polarization conversion with over 90% efficiency. At the same time, the metasurface has good angular stability up to 45°.

Keywords: Metasurface, Unit cell, Polarization, Conversion, Reflection

Yansıma Modunda Doğrusal ve Dairesel Polarizasyon için Çok Fonksiyonlu Çok Bantlı Metasurface

Öz

Çoklu ve geniş frekans bantlarında yeni bir metasurface tasarımı sunulmaktadır. Metasurface, 1.575 mm kalınlığında Roger 5880 alttas malzeme üzerine tasarlanmıştır. Tasarlanan metayüzeyin üst kısmı iki adet capraz ayna görüntülü m-şekilli birim hücreden oluşmaktadır. Arka plan düzlemi metayüzeyin tamamını kaplar. Sayısal sonuçlar, metasurface'in hem doğrusal (12,48-13,62 GHz, 19,00-27,64 GHz, 39,45-41,72 GHz, 44,68-45,18 GHz ve 47,52-48,28 GHz) hem de dairesel (11,5-12,07 GHz, 30,01-37,77 GHz, 42,3) kapasitesini göstermektedir. -44,2 GHz, 45,45-47,1 GHz, 48,7-49,54 GHz) %90'ın üzerinde verimlilikle polarizasyon dönüşümü. Aynı zamanda metayüzey 45°'a kadar iyi bir açısal stabiliteye sahiptir.

Anahtar Kelimeler: Metasurface, Birim hücre, Polarizasyon, Donusum, Yansıma

1. Introduction

The polarization of electromagnetic waves is recognized as a crucial property. Recent studies (Cheng et al., 2014; Zhang et al., 2015) focus on this property. The adjustment of the polarization state of electromagnetic waves (EM) has garnered significant attention because of its promising applications in communication, beam steering, and polarization conversions. Conventional methods such as optical gratings and dichroic crystals start to decrease their importance because they offer big wavelengths big device sizes, and narrow bands (Chen et al., 2003; Masson & Gallot, 2006). These drawbacks have steered researchers toward exploring alternative methods.

Metamaterials are artificial materials, often called metasurfaces when they're in a planar form. Metasurfaces have gained attention because they are easy to print, cost-effective, thin, and cover a wide band. These qualities make them popular in various applications due to their ability to control the phase, amplitude, and polarization state of electromagnetic waves. Metasurfaces, especially in microwave (Khan & Tahir, 2017a, 2017b; Xu et al., 2018), and terahertz (Chen et al., 2022; Zang et al., 2021; Zheng et al., 2022). have shown their effectiveness in polarization control. Their primary use lies in polarization conversion.

Polarization conversion can take different forms, like linear-to-linear (LTL) (T. Q. H. Nguyen et al., 2021; Roy et al., 2022), or linear-to-circular (LTC) (Fahad et al., 2020; Li et al., 2021). These conversions can occur either in transmission (Ako et al., 2020; Li & Zhang, 2020) or reflection mode (Cildir et al., 2023; Guo et al., 2021). In polarization conversion, certain metasurface parameters, such as efficiency, bandwidth, and angular stability, are crucial. Researchers pay close attention to these aspects when studying metasurfaces..

In the reflection mode, there have been studies (Chen et al., 2015; Lin et al., 2016; Moghadam et al., 2018) introducing metasurface-based designs for polarization conversion, achieving reported conversion efficiencies surpassing 90%. Some researchers aimed for broader bands in linear-to-linear (LTL) conversion (Shukoor et al., 2022; Yang et al., 2021). Others focused on multifunctional designs that include LTL conversion, linear-to-circular (LTC) conversion, and angular stability (Dutta et al., 2021; Tutar & Ozturk, 2022; Wahidi et al., 2020). However, even when some studies present LTC conversion, they face challenges in achieving broadband metasurfaces (Ahmed et al., 2023; Khan et al., 2019; T. K. T. Nguyen et al., 2021).

This paper introduces a new multifunctional metasurface design that operates across multiple frequency bands with broadband circular-to-linear (CTL) conversion. The designed metasurface demonstrates linear-to-linear (LTL) conversion with an efficiency exceeding 90% in frequency bands spanning 12.48-13.62 GHz, 19.00-27.64 GHz, 39.45-41.72 GHz, 44.68-45.18 GHz, and 47.52-48.28 GHz. Additionally, the metasurface achieves linear-to-circular (LTC) polarization conversion within frequency bands of 11.5-12.07 GHz, 30.01-37.77 GHz, 42.3-44.2 GHz, 45.45-47.1 GHz, and 48.7-49.54 GHz. The design also exhibits angular stability up to 45 degrees. The study covers the metasurface design, its theory and working mechanism, simulation results and discussions, and concludes with findings.

2. Material and Method

2.1. Metasurface Design

Fig. 1 depicts the designed metasurface along with the direction of the incident and reflected waves. For this design, Roger 5880 substrate with a thickness of 1.575 mm and a loss tangent of 0.009 was utilized. As shown in Fig. 1, the top of the metasurface comprises unit cells, and the back features a metallic ground plane. The unit cells are formed by two diagonal mirror m-shaped structures, with dimensions h : 1.575, s : 5, l : 4.4, w : 2.4, and g : 0.26.

As illustrated in Fig. 1, when a y-polarized wave impinges, it reflects as a y-polarized wave. Conversely, a y-polarized incident wave can be reflected as an x-polarized wave. Similarly, it is possible to reflect an x-polarized incident wave as a y-polarized wave.

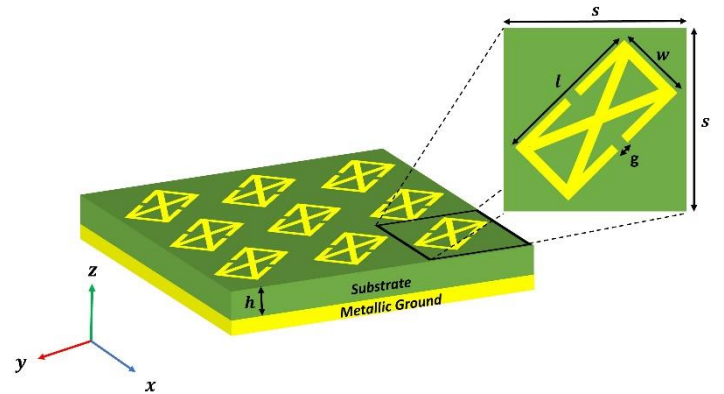


Fig. 1. Schematic view of the designed metasurface

To symbolize the incident waves and the reflected waves, the incident y- and x-polarized waves can be represented as E_{yi} , and E_{xi} , respectively. The reflected y- and x-polarized waves can be denoted E_{yr} and E_{xr} , respectively.

The relationship between the incident and reflected waves can be formulated using the following equations: $R_{yy} = |E_{yr}/E_{yi}|$, $R_{xy} = |E_{xr}/E_{yi}|$, $R_{xx} = |E_{xr}/E_{xi}|$, and $R_{yx} = |E_{yr}/E_{xi}|$.

Here, R_{yy} , and R_{xx} stand for co-coefficients of y- and x- polarized waves, respectively. R_{xy} , and R_{yx} stand for cross-coefficients of y- and x- polarized waves, respectively.

2.1.1. Metasurface Theory

In Fig. 2, the designed unit cell and the incident and reflected polarized waves are depicted in the anisotropic (uv -) coordinate system. It is evident from Figure 2 that the unit cell exhibits symmetry along the u - and v - axes. The incident (\mathbf{E}_i) and reflected (\mathbf{E}_r) polarized waves are formulated in Equ.1 and 2. Vector symbols are represented with arrows or bold fonts.

$$\mathbf{E}_i = \vec{y}E_i = \vec{u}E_{iu}e^{j\varphi_{iu}} + \vec{v}E_{iv}e^{j\varphi_{iv}} \quad (1)$$

$$\mathbf{E}_r = \vec{u}E_{ru}e^{j\varphi_{ru}} + \vec{v}E_{rv}e^{j\varphi_{rv}} \quad (2)$$

Here, E_{iu} , and E_{iv} , represent u -, and v - polarized incident waves, while E_{ru} , and E_{rv} represent u -, and v - polarized reflected waves. The symbol φ denotes the phase of these polarized waves.

Upon analyzing Equ. 1 and 2, it is expected that $|R_{uu}|$ and $|R_{vv}|$ are approximately equal to 0 dB

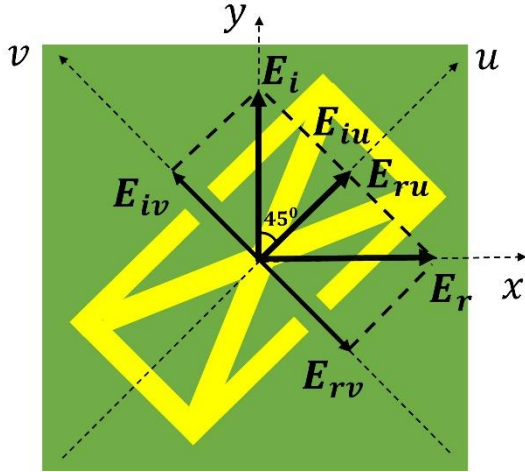


Fig. 2. The designed unit cell in the anisotropic coordinate system

To obtain LTC conversion, Equ. 3 and 4 must be provided. So, the magnitude of the co- and cross-coefficients must be equal to each other and also, their phase difference must be equal to ± 90 degrees or its multiple.

$$|R_{yy}| = |R_{xy}| \quad (3)$$

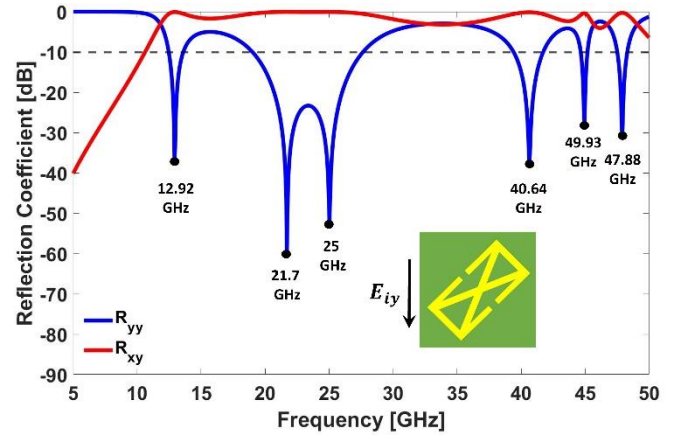
$$\Delta\varphi_{xy} = \varphi_{xx} - \varphi_{yx} = \pm\pi/2 \quad (4)$$

3. Simulation Results and Discussions

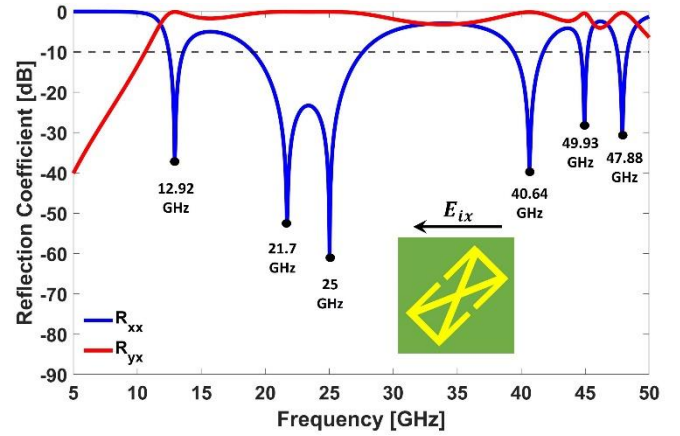
The reflection coefficient results for y-, and x-polarized waves are given in Fig. 3. The resonance frequency outcomes for y-, and x- polarized waves are observed to be identical. Additionally, it is seen that the magnitudes of reflection coefficients for the two polarized waves are almost identical due to the mirror symmetry in the anisotropic coordinate system.

For LTL conversion, co-polarized coefficients should be below -10 dB, while the cross-polarized coefficients should be close to 0 dB (Pozar, 2000). As analyzed in Fig.3, it is seen that the design has a lot of resonance frequencies and LTL conversion across multiple frequency bands.

For LTC conversion, as stated in Equ. 3, co- and cross-components should be almost equal to each other.



(a)



(b)

Fig. 3. Reflection coefficient simulation results for (a) y-polarized wave, (b) x-polarized wave

To gain a detailed understanding of LTL conversion, it is pertinent to analyze Fig. 4. In Fig. 4, the results of the polarization conversion ratio (PCR) are presented. PCR results show the efficiency of LTC conversion and can be calculated using Equ. 5.

$$PCR = \frac{|R_{xy}|^2}{|R_{xy}|^2 + |R_{yy}|^2} \quad (5)$$

As seen in Fig. 4 (a), it is understood that the metasurface converts incident wave as a linearly polarized wave within frequency bands of 12.48-13.62 GHz, 19.00-27.64 GHz, 39.45-41.72 GHz, 44.68-45.18 GHz, and 47.52-48.28 GHz over than 90 % efficiency.

Fig. 4 (b) shows the PCR angular stability of the metasurface. As the angles change, variations in the efficiency of the metasurface are observed. The designed metasurface is capable of performing Linear-to-Circular (LTC) conversion with a certain level of efficiency up to 45 degrees.

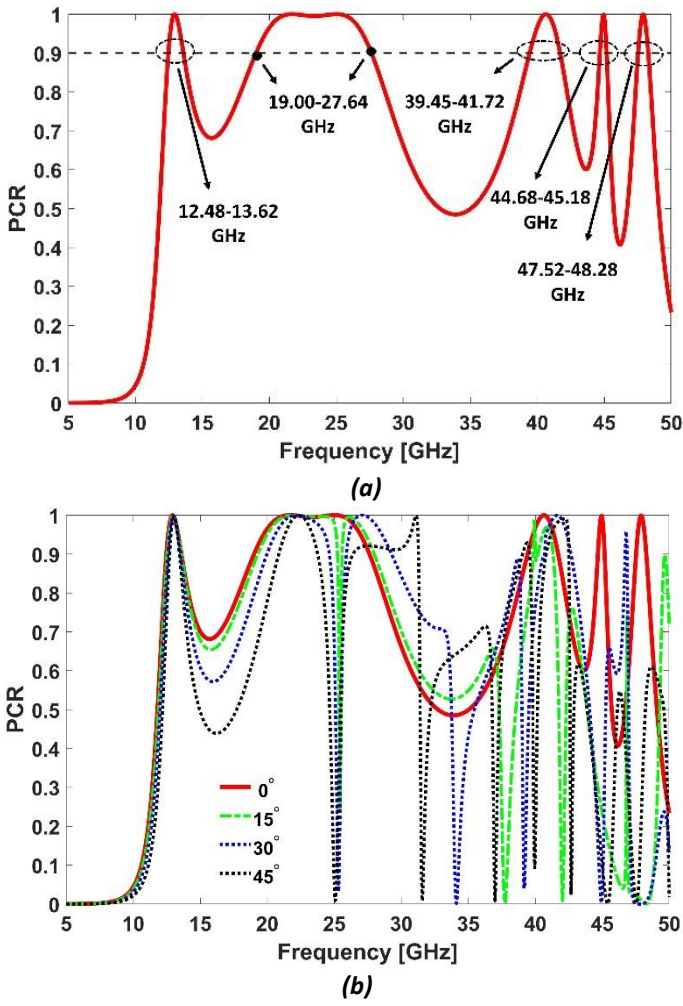


Fig. 3. PCR simulation results for: (a) normal incidence (0 degree), (b) different angles

To validate LTC conversion, the axial ratio (AR) can be analyzed. AR helps us discover circular polarization conversion.

$$AR_{dB} = 10 \log \left| \frac{R_{xy}}{R_{xx}} \right| \quad (6)$$

Axial ratio simulation results are depicted in Fig. 4. According to Equ. 4, and 6, the axial ratio results falling between -3 and +3 dB can be considered thresholds for LTC conversion. Fig. 4 shows the frequency band regimes where LTC conversion occurs for a normal incidence wave (0 degrees).

Fig 4 (b) also demonstrates that the metasurface can make LTC conversion with different angles. The different angles in the axial ratio graph show that the metasurface exhibits angular stability up to 45 degrees. Hence, this metasurface has the capability to convert circular polarization across various frequencies for different angles.

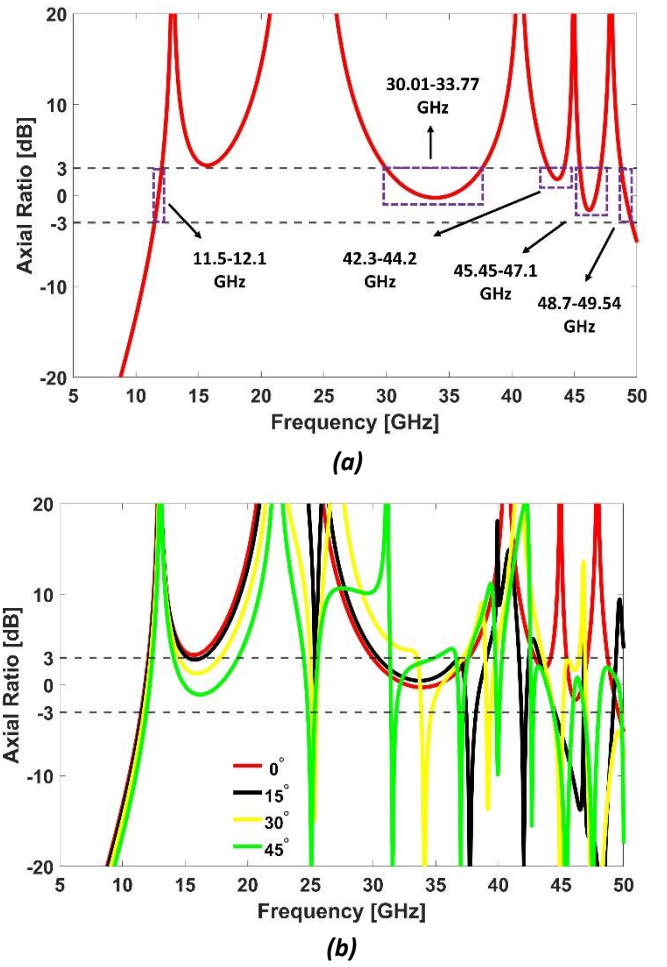


Fig. 4. Axial ratio simulation results for (a) normal incidence (0 degrees), and (b) different angles.

4. Conclusion

In this paper, a new multi-functional, multi-broadband metasurface design has been presented. The metasurface effectively converts linear x- and y-polarized waves to linear y- and x-polarized waves within frequency bands spanning 12.48-13.62 GHz, 19.00-27.64 GHz, 39.45-41.72 GHz, 44.68-45.18 GHz, and 47.52-48.28 GHz, achieving an efficiency exceeding 90%. This metasurface can also do LTC conversion in frequency bands of 11.5-12.07 GHz, 30.01-37.77 GHz, 42.3-44.2 GHz, 45.45-47.1 GHz, 48.7-49.54 GHz. Moreover, this design includes angular stability up to 45°. Future studies can focus on wider frequency bands for LTL and LTC conversion.

References

- [1] Ahmed, A., Cao, Q., Khan, M. I., Ahmed, F., & Tahir, F. A. (2023). A multifunctional broadband polarization rotator based on reflective anisotropic metasurface. *Physics Letters A*, 470, 128785.
- [2] Ako, R. T., Lee, W. S., Atakaramians, S., Bhaskaran, M., Sriram, S., & Withayachumnankul, W. (2020). Ultra-wideband tri-layer transmissive linear polarization converter for terahertz waves. *APL Photonics*, 5(4).
- [3] Chen, B., Wang, X., Li, W., Li, C., Wang, Z., Guo, H., Wu, J., Fan, K., Zhang, C., & He, Y. (2022). Electrically addressable

- integrated intelligent terahertz metasurface. *Science Advances*, 8(41), eadd1296.
- [4] Chen, C.-Y., Tsai, T.-R., Pan, C.-L., & Pan, R.-P. (2003). Room temperature terahertz phase shifter based on magnetically controlled birefringence in liquid crystals. *Applied Physics Letters*, 83(22), 4497-4499.
- [5] Chen, H.-Y., Wang, J.-F., Ma, H., Qu, S.-B., Zhang, J.-Q., Xu, Z., & Zhang, A.-X. (2015). Broadband perfect polarization conversion metasurfaces. *Chinese Physics B*, 24(1), 014201.
- [6] Cheng, Y. Z., Withayachumnankul, W., Upadhyay, A., Headland, D., Nie, Y., Gong, R. Z., Bhaskaran, M., Sriram, S., & Abbott, D. (2014). Ultrabroadband reflective polarization converter for terahertz waves. *Applied Physics Letters*, 105(18).
- [7] Cildir, A., Tahir, F. A., Imran, M., & Abbasi, Q. (2023). An Innovative Metasurface Polarizer Working in 5G Frequency Bands.
- [8] Dutta, R., Ghosh, J., Yang, Z., & Zhang, X. (2021). Multi-band multi-functional metasurface-based reflective polarization converter for linear and circular polarizations. *IEEE Access*, 9, 152738-152748.
- [9] Fahad, A. K., Ruan, C., Nazir, R., Saleem, M., Haq, T. U., Ullah, S., & He, W. (2020). Ultra-thin metasheet for dual-wide-band linear to circular polarization conversion with wide-angle performance. *IEEE Access*, 8, 163244-163254.
- [10] Guo, Y., Xu, J., Lan, C., & Bi, K. (2021). Broadband and high-efficiency linear polarization converter based on reflective metasurface. *Engineered Science*, 14(2), 39-45.
- [11] Khan, M. I., Khalid, Z., & Tahir, F. A. (2019). Linear and circular-polarization conversion in X-band using anisotropic metasurface. *Scientific reports*, 9(1), 4552.
- [12] Khan, M. I., & Tahir, F. A. (2017a). An angularly stable dual-broadband anisotropic cross polarization conversion metasurface. *Journal of Applied Physics*, 122(5).
- [13] Khan, M. I., & Tahir, F. A. (2017b). Simultaneous quarter-wave plate and half-mirror operation through a highly flexible single layer anisotropic metasurface. *Scientific reports*, 7(1), 16059.
- [14] Li, S., & Zhang, X. (2020). Asymmetric tri-band linear-to-circular polarization converter in transmission mode. *International Journal of RF and Microwave Computer-Aided Engineering*, 30(2), e21959.
- [15] Li, Z., Yang, R., Wang, J., Zhao, Y., Tian, J., & Zhang, W. (2021). Multifunctional metasurface for broadband absorption, linear and circular polarization conversions. *Optical Materials Express*, 11(10), 3507-3519.
- [16] Lin, B., Wang, B., Meng, W., Da, X., Li, W., Fang, Y., & Zhu, Z. (2016). Dual-band high-efficiency polarization converter using an anisotropic metasurface. *Journal of Applied Physics*, 119(18).
- [17] Masson, J.-B., & Gallot, G. (2006). Terahertz achromatic quarter-wave plate. *Optics letters*, 31(2), 265-267.
- [18] Moghadam, M. S. J., Akbari, M., Samadi, F., & Sebak, A.-R. (2018). Wideband cross polarization rotation based on reflective anisotropic surfaces. *IEEE Access*, 6, 15919-15925.
- [19] Nguyen, T. K. T., Nguyen, T. M., Nguyen, H. Q., Cao, T. N., Le, D. T., Bui, X. K., Bui, S. T., Truong, C. L., Vu, D. L., & Nguyen, T. Q. H. (2021). Simple design of efficient broadband multifunctional polarization converter for X-band applications. *Scientific reports*, 11(1), 2032.
- [20] Nguyen, T. Q. H., Nguyen, T. K. T., Nguyen, T. Q. M., Cao, T. N., Phan, H. L., Luong, N. M., Le, D. T., Bui, X. K., Truong, C. L., & Vu, D. L. (2021). Simple design of a wideband and wide-angle reflective linear polarization converter based on crescent-shaped metamaterial for Ku-band applications. *Optics Communications*, 486, 126773.
- [21] Pozar, D. M. (2000). *Microwave and RF design of wireless systems*. John Wiley & Sons.
- [22] Roy, K., Sinha, R., & Barde, C. (2022). Linear-to-linear polarization conversion using metasurface for X, Ku and K band applications. *Frequenz*, 76(7-8), 461-470.
- [23] Shukoor, M. A., Dey, S., & Koul, S. K. (2022). Broadband chiral-type linear to linear reflecting polarizer with minimal bandwidth reduction at higher oblique angles for satellite applications. *IEEE Transactions on Antennas and Propagation*, 70(7), 5614-5622.
- [24] Tutar, F., & Ozturk, G. (2022). An effective metasurface-based linear and circular polarization converter for C-and X-band applications. *Optical Materials*, 128, 112355.
- [25] Wahidi, M. S., Khan, M. I., Tahir, F. A., & Rmili, H. (2020). Multifunctional single layer metasurface based on hexagonal split ring resonator. *IEEE Access*, 8, 28054-28063.
- [26] Xu, J., Li, R., Wang, S., & Han, T. (2018). Ultra-broadband linear polarization converter based on anisotropic metasurface. *Optics Express*, 26(20), 26235-26241.
- [27] Yang, X., Ding, Z., & Zhang, Z. (2021). Broadband linear polarization conversion across complete Ku band based on ultrathin metasurface. *AEU-International Journal of Electronics and Communications*, 138, 153884.
- [28] Zang, X., Yao, B., Chen, L., Xie, J., Guo, X., Balakin, A. V., Shkurinov, A. P., & Zhuang, S. (2021). Metasurfaces for manipulating terahertz waves. *Light: Advanced Manufacturing*, 2(2), 148-172.
- [29] Zhang, L., Zhou, P., Chen, H., Lu, H., Xie, J., & Deng, L. (2015). Adjustable wideband reflective converter based on cut-wire metasurface. *Journal of Optics*, 17(10), 105105.
- [30] Zheng, C., Li, J., Liu, L., Li, J., Yue, Z., Hao, X., Zhang, Y., Zang, H., & Yao, J. (2022). Optically tunable terahertz metasurface absorber. *Annalen der Physik*, 534(5), 2200007.